Neurobiology of Disease 126 (2019) 105–116

Contents lists available at ScienceDirect

Neurobiology of Disease

journal homepage: www.elsevier.com/locate/ynbdi

Review

Decline in Sirtuin-1 expression and activity plays a critical role in blood-brain barrier permeability in aging

Svetlana M. Stamatovic[a], Gabriela Martinez-Revollar[a], Anna Hu[a], Jennifer Choi[a], Richard F. Keep[b,c], Anuska V. Andjelkovic[a,b,*]

[a] Department of Pathology, Medical School, University of Michigan, Ann Arbor, MI 48109, USA
[b] Department of Neurosurgery, Medical School, University of Michigan, Ann Arbor, MI 48109, USA
[c] Molecular and Integrative Physiology, University of Michigan Medical School, Ann Arbor, MI 48109, USA

ARTICLE INFO

Keywords:
Blood-brain barrier
Permeability
Aging
Tight junction
Sirtuin-1

ABSTRACT

Accumulating evidence suggest that cerebral microvascular disease increases with advancing age and is associated with lacunar stroke, leukoaraiosis, vascular dementia and Alzheimer disease. Increased blood brain barrier (BBB) permeability/leakage takes “center stage” in ongoing age-related vascular/brain parenchymal injury. Although significant effort has been made in defining the gene mutations and risk factors involved in microvascular alterations in vascular dementia and Alzheimer disease, the intra- and intercellular pathogenic mechanisms responsible for vascular hyperpermeability are still largely unknown. The present study aimed to reveal the ongoing senescence process in brain endothelial cells and its effect on BBB integrity in healthy/non-disease conditions. An analysis of BBB integrity during the life span of C56Bl6 mice (young, 2–6 months; middle-aged, 6–12, months; old, 16–22 months) showed increased BBB permeability for different molecular sized tracers (sodium fluorescein, inulin and 20 kDa dextran) in aged mice which was accompanied by modifications in tight junction (TJ) complex organization, manifested as altered TJ protein expression (particularly claudin-5). A gene screening analysis of aging associated markers in brain microvessels isolated from “aged” mice (C56Bl6, 18-20 months) and human brain samples showed a significant decline in sirtuin-1 expression (Sirt1; ~2.8-fold) confirmed at mRNA and protein levels and by activation assay. Experiments in Sirt1 transgenic mice and brain endothelial cell-specific Sirt1 knockout mice indicated that Sirt1 affects BBB integrity, with loss increasing permeability. Similarly, in vitro, overexpressing Sirt1 or increasing Sirt1 activity with an agonist (Sirt1720) protected against senescence-induced brain endothelial barrier hyperpermeability, stabilized claudin-5/ZO-1 interactions and rescued claudin-5 expression. These findings reveal a novel role of Sirt1 in modulating aging-associated BBB persistent leakage.

1. Introduction

Gradual increases in human lifespan have resulted in an epidemic-like increase in aging-associated diseases (i.e. cardiovascular, neurodegenerative and metabolic diseases). Aging itself results in well-defined phenotypic changes, which render the cerebro- and cardiovascular systems prone to disease, even in the absence of traditional risk factors (e.g. hypertension, diabetes, and smoking) (Farrall and Wardlaw, 2009; Pantoni, 2010). Cerebrovascular alterations include reduced microvascular density, particularly in hippocampus, white matter and cortex, loss of angiogenic capacity and microvascular plasticity (Brown and Thore, 2011; Grinberg and Thal, 2010). The main characteristic of aging microvessels is degeneration affecting the cerebral endothelium, manifested as degenerative and focal necrotic changes, decreased mitochondrial content, increased pinocytotic vesicles, loss of tight junctions (TJs), decreased number of pericytes and swollen astrocytic end-feet and thickening of the basal lamina (Grinberg and Thal, 2010; Richardson et al., 2012; Rouhl et al., 2012; Wardlaw, 2008). As a consequence, there is focally compromised blood-brain barrier (BBB) integrity. It has been thought that increased BBB permeability (BBB leakage) in aging is a secondary event, developing as a consequence of processes like inflammation, atherosclerosis, impaired autoregulation, microthrombosis and amyloid deposition (Farrall and Wardlaw, 2009; Simpson et al., 2010; Wardlaw et al., 2008). However,

* Corresponding author at: Department of Pathology and Neurosurgery, Medical School, University of Michigan, 7520A MSRB I, 1150 W Medical Center Dr, Ann Arbor, MI 48109, USA.
E-mail address: anuskaa@med.umich.edu (A.V. Andjelkovic).

https://doi.org/10.1016/j.nbd.2018.09.006
Received 27 May 2018; Received in revised form 20 August 2018; Accepted 5 September 2018
Available online 06 September 2018
0969-9961/

several recent clinical MRI studies indicate that BBB leakage could be a primary cause for the development of vascular/brain parenchymal injury seen in the aging brain (Gorelick et al., 2011; Heye et al., 2014; Simpson et al., 2010; Wardlaw et al., 2008).

The BBB is a highly complex and dynamic barrier, formed by an interdependent network of brain capillary endothelial cells, endowed with barrier properties, and perivascular cells (astrocytes and pericytes) responsible for inducing and maintaining the barrier (Abbott et al., 2010). Normally, the BBB paracellular pathway is highly impermeable due to the presence of a junctional (tight, adherens and gap) complex. The TJ complex has the major role in occluding the paracellular space between brain endothelial cells and determining the BBB physical properties (Stamatovic et al., 2016). The complex is built by intricate interactions between three components: transmembrane proteins (claudin-5, occludin, JAM-A), important for occluding the paracellular space, scaffolding proteins (ZO-1,-2, VASP) and the actin cytoskeleton vital for physical support and junction function (Gonzalez-Mariscal et al., 2003; Stamatovic et al., 2016). Any defect in these components, affects the stability and adhesive interactions of junctional proteins, increasing paracellular permeability (BBB leakage).

As to the cause of BBB hyperpermeability in aging, limited clinical and experimental studies have primarily focused on potential factors at the neurovascular unit, which may alter BBB permeability (Bell and Zlokovic, 2009; Guerriero et al., 2017; Halliday et al., 2016; Yamazaki et al., 2016). Changes in the number of pericytes and morphological changes in astrocyte interactions at BBB, and ongoing inflammatory processes are considered critical for loss of BBB integrity (Bell and Zlokovic, 2009; Guerriero et al., 2017; Halliday et al., 2016; Kaur et al., 2011). Although BBB leakage might be a response to microenvironment changes in aging brain parenchyma, an important part involves “aging” processes in the brain endothelial cell and brain endothelial barrier, which could be a primary trigger of pathological cerebrovascular changes (Ueno et al., 1993; Yamazaki et al., 2016; Yang et al., 2018). How brain endothelial cells and the barrier “age” and which potential factors are involved in this process are still unclear.

One emerging factor associated with a decline of endothelial cell function in aging is Sirtuin1 (Sirt1). Sirt1 is a nicotinamide adenine dinucleotide (NAD) + dependent class III histone deacetylase, involved in a myriad of cell functions (i.e. cellular metabolism, stress response, cell cycle, senescence, death pathways) (Chang and Guarente, 2014; Imai and Guarente, 2014). Sirt1, the most common expressed sirtuin in mammalian brain, is engaged in cross-talk with several signaling pathways, deacetylation of numerous transcription factors and co-factors (i.e. p53, E2F1, NFκB, FOXO), chromatin remodeling, regulating cellular processes and gene expression. It is at the interface of oxidative stress, inflammation and apoptosis responses (Hori et al., 2013; Kauppinen et al., 2013; Mouchiroud et al., 2013). Sirt1 activity is involved in brain development, regulating circadian rhythm, endocrine function, feeding behavior and neuronal plasticity as well modulating cognitive function and aging associated neuronal degeneration (Chang and Guarente, 2014; Imai and Guarente, 2014).

Several lines of evidence suggest that Sirt1 also acts as a longevity factor in vascular tissue (Koronowski et al., 2017; Li et al., 2014; Tajbakhsh and Sokoya, 2012). Activation of Sirt1 can also prevent endothelial senescence, reduce endothelial atherosclerotic lesions during elevated lipid states and prevent oxidative injury (Chen et al., 2015; Ding et al., 2015; Yang et al., 2012). Although there are an increasing number of studies on the involvement of Sirt1 brain and peripheral vasculature aging, there is a lack of evidence on the potential role of Sirt1 in BBB aging. The current study focused on defining the effect of senescence processes in brain endothelial cells on BBB integrity in healthy/non-disease conditions and in defining the role of Sirt1 in aging-induced BBB ‘leakage”.

2. Methods

2.1. Animals

All experimental procedures were approved by The Institutional Animal Care and Use Committee, University of Michigan, Medical School. Experiments were performed on male and female mice assigned to three age groups: young (3–6 months), middle (8–16 months) and old age (18–24 months) strain C56Bl/6 (Charles River and National institute of aging, NIA colony). In addition, Sirt1 Tg mice ($SirT1^{super}$, C57BL/6xCBA, Jackson laboratory), $SirT1^{flox/flox}$ mice (C57B6;129-$Sirt1^{tm1Ygu/J}$) and claudin-5 cre mice ($Cldn5^{icre}$ C57BL/6, generous gift for Elisabeth Simpson, University of British Columbia) were used. $SirT1^{flox/flox}$ and homozygous $Cldn5^{icre}$ were crossed to obtain brain endothelial conditional Sirt1 knockout mice.

2.2. Brain tissue

Human postmortem brain tissue samples were obtained from the Human Brain and Spinal Fluid Resource Center (West Los Angeles Healthcare Center, Los Angeles, USA) and Mount Sinai NBTR (New York USA), which is, sponsored by NINDS/NIMH, National Multiple Sclerosis Society and Department of Veteran Affairs. Control brain slides were obtained from ProSci Incorporated and had no stroke pathology. Details of the brain samples utilized in this study are included in Supplementary Table S1. Ethical approval for these studies was obtained from the Institution Review Board, University of Michigan Medical School. Fresh frozen tissue was used for RT-PCR analysis or was fixed with 4% paraformaldehyde and cut at 15 μm, while paraffin-embedded brain tissue was cut at 4 μm and used for immunohistochemistry.

2.3. Mouse endothelial cell culture

Mouse brain microvascular endothelial cells (mBMEC) were prepared using a modified protocol already described (Stamatovic et al., 2006; Stamatovic et al., 2003). Briefly, brains were collected from four to six-week-old C57BL/6 mice, minced and homogenized gently in a Dounce type homogenizer in Hank's balance solution (HBSS, Thermo Fisher Scientific). Myelin was removed by resuspending homogenates in 18% Dextran suspension (Dextran 60–90,000; USB,) and centrifuging. Red blood cells were removed by centrifuging isolated microvessels in a Percoll gradient (Pharmacia) at 2700 rpm for 11 min. The isolated microvessels were digested by collagenase/dispase (1 μg/ml, Roche), and precipitated with CD31 coated magnet beads (Dynabeads, Thermo Fisher Scientific). These vessels were further cultured in growth media. This protocol typically produces primary endothelial cell cultures that are approximately 99% pure (as determined by immunocytochemistry with an anti-PECAM-1 antibody; BD Bioscience).

2.4. In vitro aging model

In vitro, “aging/senescence” was achieved by continually passaging primary brain endothelial cells (mBMEC). Briefly isolated primary mBMEC were grown in brain endothelial growth media (DMEM), 10% Fetal bovine serum, 2.5 μg/ml heparin (Sigma), 20 mM HEPES, 2 mM glutamine, 1× antibiotic/antimycotic (Thermo Fisher Scientific) at 37 °C in a humidified incubator with 5% CO_2. mBMEC were passaged when monolayers reached 75–90% confluence. For each passage, cell number and senescence marker expression were determined. The number of population doublings [(PDs), PD = $\log_2$(number of cells proliferated/number of cells seeded] and cumulative population doubling level (CPDL), which represent the age of the mBMEC in vitro, were determined (Lee et al., 2010). For mBMEC, complete senescence was achieved at CPDL = 6. Senescence was verified by the expression of senescence-associated β-galactosidase, using sen-β-gal assay (Cell

Signaling Technology), high expression of senescence-associated marker cyclin-dependent kinase inhibitor 1A (Cdkn1a/p21), marker for DNA damage γH2A.X evaluated by immunofluorescence and Western blotting using the corresponding antibodies (Abcam) and senescence-associated heterochromatin foci (SAHF) labeled by DAPI staining. Based on the correlation of these factors and CPDL, mBMEC were divided into three stages young, intermediate, and senescent with CPDLs of 1, 3 and 6. Chemically-induced senescence was achieved by treating mBMEC with 200 μM H_2O_2, (Sigma) for 2 h in DMEM media without serum following the replacement with growth media for an additional 24 h. Senescence was verified by sen-β-gal assay, and expression of p21, γH2A.X as well the presence of SAHF in the cell nucleus.

2.5. Cell treatment

Sirt1 depletion was achieved through transfection with Sirt1 siRNAs (#si174219 #174220, #174221, Thermo Fisher Scientific) targeting 3 different regions of Sirt1. As controls, cells were transfected with control siRNA (sicontrol #2, Thermo Fisher Scientific). Sirt1 activity was also decreased by exposure to Sirt1 inhibitor Ex527 (1 μM, Tacom) or increased using the Sirt1 agonist SRT1720. Transcellular permeability was inhibited by treating cells with Fillipin III (Sigma Aldrich).

2.6. Gene array analysis

Total RNA from the human and mouse brain microvessels was prepared using TRIZOL (Thermo Fisher Scientific). Single strand cDNA was synthesized using RT^2 first strand kit (Qiagene). Analysis of senescence marker mRNA expression in human and mouse brain microvessels was done using Human and Mouse Aging PCR-array (Qiagen), according to the manufacturer's protocol. The mRNA expression pattern was evaluated using software provided by the manufacturer.

Analysis of Sirt1 mRNA expression in microvessels isolated from human and mouse brain tissue as well as in mBMEC, was performed using TaqMan real-time PCR assay on Applied Biosystem 7500 Real time PCR system (Applied Biosystems). Single strand cDNA was synthesized using RT^2 first strand kit (Qiagen). Real-Time PCR was performed for SirT1 using commercially available primers (Qiagen). β-actin was used to normalize the amount of SirT1 mRNA in each sample.

2.7. Permeability assay

In vivo BBB integrity was assessed by determining the transfer coefficient or permeability index (K_i) for sodium fluorescein (376 Da), FITC-dextran 3 kDa, FITC-dextran (20 kDa), as described previously in our laboratory. The permeability of mBMEC monolayers in vitro was measured as described in Kazakoff et al., and modified in our laboratory (Kazakoff et al., 1995; Sladojevic et al., 2014). The permeability coefficient (PC; cm/min) of monolayers was calculated for the tracers FITC-inulin or dextran-Texas red (1 μg/ml, Sigma-Aldrich).

Transcellular permeability of mBMEC monolayers in a Transwell chamber system (0.4 μm pore size) was assessed using Alexa Fluor 647-bovine serum albumin (BSA). The tracer (10 μg/ml) was loaded in the insert chamber. Transendothelial permeability was measured by determining the albumin concentration in bottom chamber which was calculated from a standard curve.

2.8. Transendothelial electrical resistance (TEER) measuring

The TEERs of mBMEC monolayers were measured with an Endohom-12 electrical resistance apparatus (World Precision Instruments Inc., Sarasota, FL, U.S.A.). The resistance of a blank filter was subtracted to calculate final TEER values ($\Omega.cm^2$). All experiments were carried out in triplicate. The results were expressed as means ± SE of five independent experiments.

2.9. Sirt1 activation assay

Sirt1 activity was evaluated using a Sirt1 activity assay kit (Abcam) in mBMEC in vitro and in isolated brain microvessels. The assay was performed according to the manufacturer's instructions.

2.10. Immunofluorescence and quantitative immunofluorescence

For immunofluorescence staining, brain section and cell samples were preincubated in blocking solution containing 5% normal horse serum and 0.05% Triton 100× (Sigma-Aldrich) in PBS. Samples were then incubated overnight at 4 °C with the following primary antibodies: anti-claudin-5 Alexa-Fluor 488 conjugated, ZO-1-Alexa Fluor 594 conjugated (both from Thermo Fisher), anti-Sirt1 (Cell Signaling Technology), and anti-fibrinogen (Abcam). Reactions were visualized by anti-rabbit, anti-mouse fluorophore conjugated antibodies (Vector Laboratories) or anti-sheep (R&D System). All samples were viewed on a confocal laser scanning microscope (Nikon A1, Japan).

To evaluate fibrinogen extravasation due to BBB leakage in human brain tissue samples, four sections per case and control slides in region of frontal cortex and basal ganglia were chosen and on each histological slide ten spots were randomly selected. Images (40 images per each staining) for fibrinogen quantitative florescence analysis were acquired on a confocal laser-scanning microscope (Nikon A1, Japan) with sequential mode to avoid interference between channels and saturation. Contrast, brightness and the pinhole were held constant. Analysis was done in ImageJ software by outlining the extravascular fibrinogen + area (area around blood vessels, fibrinogen + ve) in each image and the fluorescence intensity in the enclosed area was measured. Background intensity was subtracted from the fluorescence intensity.

2.11. Western blotting

mBMEC and isolated brain microvessels were washed with PBS and then lysed in RIPA buffer. Western blotting was performed with anti-claudin-5, -ZO-1, -Sirt1, −β-actin and -GAPDH antibodies (Cell Signaling Technology). Immunoblots were exposed to secondary antibodies, either anti-mouse-, or anti-rabbit-HRP conjugated antibody (BioRad) and visualized with a chemiluminescent HRP substrate kit and analyzed using Image J software.

2.12. Proximity ligation assay

Monolayers of mBMEC were washed, fixed and pre-incubated with permeabilisation solution (DPBS and 0.5% Triton X-100) for 5 min following by blocking solution (DPBS + + containing 0.5% (*v*/v) Triton X-100 and 5% goat serum). mBMEC were then incubated with primary antibody pairs (mouse anti-claudin-5 and rabbit anti-ZO-1 antibodies) for 18 h. Then the mBMEC monolayers were washed with DPBS containing 5% goat serum under gentle agitation and exposed to rabbit Plus (DUO92002) and anti-mouse Minus (DUO92004) and incubated for 1 h in a humidified incubator at 37 °C, 5% CO_2. Protein-protein interactions were detected using the Detection Kit Red (DUO92008) according to the manufacturer's (Sigma) instructions. Samples were mounted on slides using Duolink In Situ Mounting Medium with 4,6-diamidino-2-phenylindole (DUO82040) and imaged.

2.13. Statistical analysis

Analyses were performed using GraphPad Prism 6.0. Unpaired, two-tailed Student's *t*-test and one-way analysis of variance (ANOVA), with Tukey post hoc tests were used to test group level differences. Correlations were analyzed with Pearson's correlation χ^2 test. A probability value $< .05$ was regarded as statistically significant.

3. Results

3.1. BBB integrity in aging brain

Alterations in BBB integrity were observed during the life span of mice. Based on the corresponding human aging category, mice were divided into three age groups: young (2–6 months), middle aged (8–14 months) and old (16–22 months). BBB permeability was determined using four different sized tracers: sodium fluorescein (SF, 376 Da), inulin (5 kDa) and dextran (20 and 40 kDa) in brain of C56Bl/6 mouse strain, without any pathological conditions (healthy mice). The BBB was impermeable for all tested tracers in young mice but showed a steady and significant increase in clearance of SF and inulin in middle age ($p < 0.01$, SF; $p < 0.05$ inulin) and old age mice (16–22 months; $p < 0.001$ SF and inulin). The BBB was permeable to 20 kDa Dextran in old mice ($p < 0.05$; Fig. 1A). The BBB was impermeable to the high molecular weight tracer 40 kDa dextran indicating the absence of any complete BBB breakdown. No sign of water accumulation was present in all examined brain (data not showed). A correlation analysis of BBB inulin permeability with age had positive a Pearson coefficient ($r = 0.941$, $p < 0.001$) confirming that the BBB become compromised/leaky during aging in healthy mice (Fig. 1B).

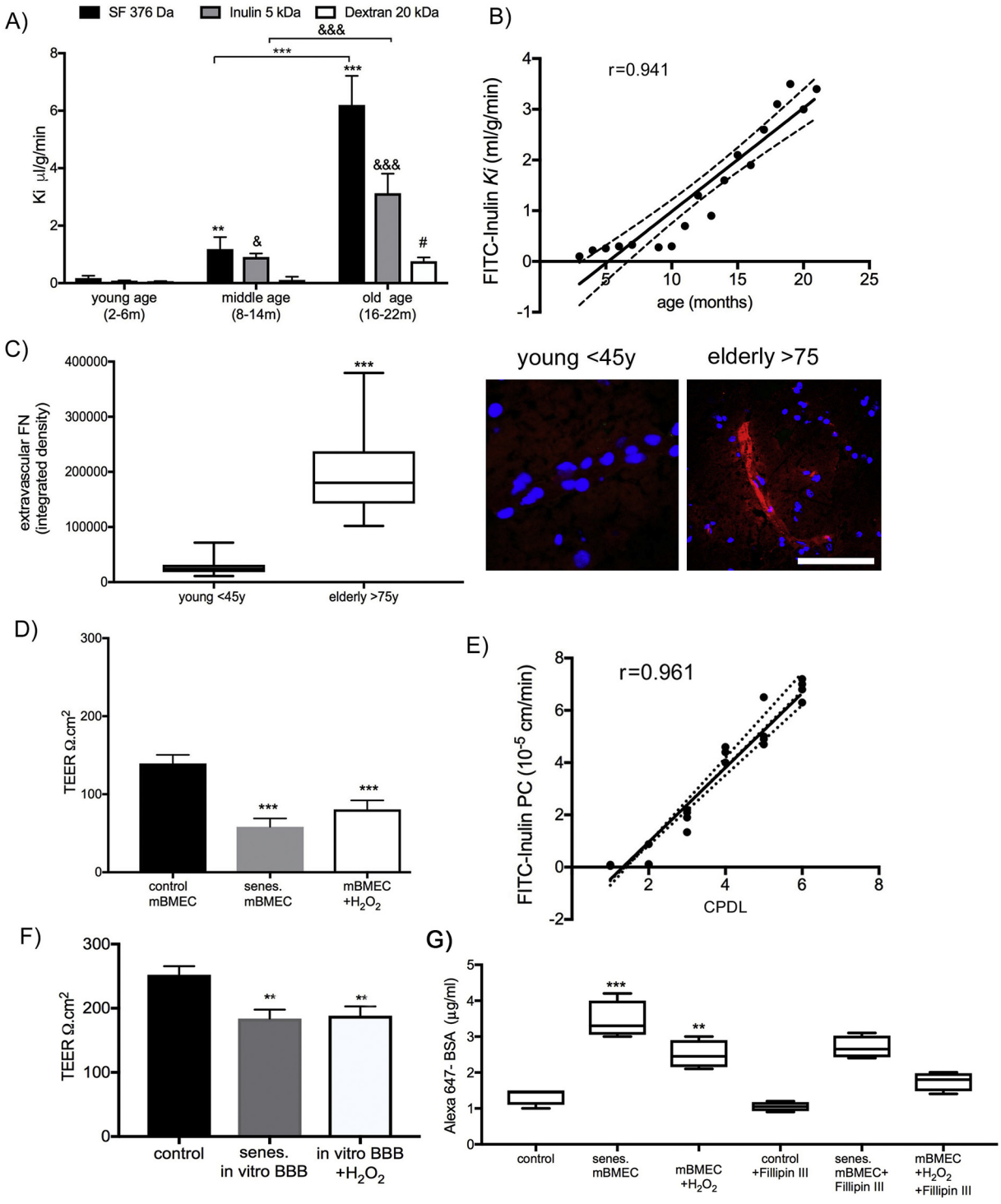

(caption on next page)

Fig. 1. Increased BBB permeability with aging. A) Influx rate constant (Ki) for sodium fluorescein (SF, 376 Da), inulin (5 kDa) and dextran 20 kDa in whole brain in young (2–6 months), middle-aged (8–14 months) and old (16–22 months) mice. Values are means ± SD, n = 6. **p < 0.01 and ***p < 0.001 for SF comparing to young age; $^{\&}$p < 0.05 and $^{\&\&\&}$ p < .001 for inulin comparing to young age; $^{\#}$p < 0.05 for dextran comparing to young age. B) Correlation between age and BBB permeability (inulin Ki). Pearson coefficient $r = 0.941$ (p < 0.001). C) Box and whisker plot represents semi-quantitation of the extravascular accumulation of serum protein fibrinogen. Analysis of two regions (basal ganglia and cortex) showed no difference in fibrinogen extravasation and the results were pooled. Values are from n = 20 analyzed blood vessels on 4 separate slides in 2 elderly cases (> 75 years) and 2 control - young cases (< 45 years). ***p < 0.001 vs. young (control) brain. Examples of fibrinogen (red) immunofluorescence from an elderly and a young brain. Blue DAPI staining indicates nuclei. Note the increased permeability of the blood vessel (leak to fibrinogen) in the elderly brain. Scale bar 50 μm. D) Senescent mBMEC monolayers induced by continuous passage of cells or treatment with 100 μM H_20_2 had reduced transendothelial electrical resistance (TEER) Values are means ± SD, n = 5; ***p < 0.001 comparing to control mBMEC monolayer. E) Correlation between degree of senescence of the brain endothelial cells induced by cumulate population doubling level (CPDL) and the barrier permeability coefficient (PC) for inulin. Pearson coefficient r = 0.961; p < 0.001. F) Co-culture of astrocytes with mBMEC (in vitro BBB) results in a higher TEER than monoculture alone. This is reduced by chemically induced senescence (exposure of mBMEC and astrocytes to 100 μM H_20_2). Values are means ± SD, $n = 5$; **p < 0.01, comparing to control in vitro BBB. G) Transcellular permeability of mBMEC monolayer for tracer Alexa647-BSA. The tracer was added to upper chamber of Transwell dual chamber system and concentration of Alexa Fluor 647-bovine serum albumin (BSA) was measured in lower chamber. Fillipin III (5 μg/ml) - inhibitor of caveolae formation was added and beginning of assay. Values are means ± SD, n = 3; **p ≤ 0.01, ***p ≤ 0.001, comparing to control mBMEC. (For interpretation of the references to colour in this figure legend, the reader is referred to the web version of this article.)

A parallel analysis of BBB integrity in "young" (< 45 years old) and "elderly" (> 75 years old) human brain showed a similar change with age. The BBB was evaluated by examining fibrinogen extravasation in two brains from elderly patients (over age of 75 years with a medical history of cardiovascular and cerebrovascular diseases and two control brain samples from young patients, < 45 years old) (Supplementary Table S1). Brain samples from elderly patients, but not young patients, presented with robust fibrinogen extravasation and accumulation (Fig. 1C). Semi-quantitative analysis showed high level of extravascular fibrinogen in aged patients, indicating a compromised BBB (p < 0.001; Fig. 1C).

As changes in BBB permeability with age could reflect alterations in the neurovascular unit, we modeled senescence in vitro. Senescence of mouse brain microvascular endothelial cell (mBMEC) monolayers and astrocytes was achieved through continuous passage (Supplementary Fig. S1A). Due to the complexity of the processes involved in senescence, barrier alterations in aging were studied in two senescence model systems, continuous propagation (replicative senescence) and exposure to subtoxic dose of H_2O_2 (chemical senescence). The replicative senescence is characterized with shortening telomeres mostly seen in situ aging cells (Chang and Harley, 1995). Besides the shortening of telomeres, senescence is characterized by increased production and incompetent control of reactive oxygen species, which have damaging effects on biomolecules (e.g. DNA damage), decline in tissue function and premature aging (Chen et al., 1995; Dierick et al., 2002; Dimri et al., 1995).

In our model system, complete senescence occurred at CPDL = 6 in mBMEC and CPDL = 12 in astrocytes with appearance and progressive expression of senescence-associated β-galactosidase (sen-β-gal+), senescence-associated marker cyclin-dependent kinase inhibitor 1A (Cdkn1a/p21+), marker for DNA damage (γH2A.X+) and senescence-associated heterochromatin foci (SAHF+) (p ≤ 0.01 and p ≤ 0.001, Pearson correlation coefficients between CPDL and senescence markers for mBMEC ad astrocytes (Supplementary Fig. S1 A). Senescence was also achieved by treatment with H_2O_2 (chemical- oxidative stress induced senescence) where cells showed similar pattern in expression of all senescence markers in mBMEC and astrocytes (Supplementary Fig. S1 B). With senescence, the brain endothelial barrier had decreased TEER values (Fig. 1D) and increased inulin permeability (Fig. 1E). In particular, there was a positive correlation between mBMEC monolayer permeability and the number of passages, which represent the stage of the senescence (Pearson coefficient, $r = 0.961$, p ≤ 0.001; Fig. 1E). The presence of senescence astrocytes in the in vitro BBB model, did not have protective effect on barrier integrity; suggesting that endothelial, as well senescence of components in the neurovascular unit, are both critical for compromised BBB integrity found with aging (Fig. 1F).

In addition to paracellular permeability, "aging" process affected transcellular barrier permeability. Senescence, via passage or H_2O_2 treatment of mBMEC monolayers, showed increased permeability of Alexa Fluor 647-bovine serum albumin (mol. wt. ~70 kDa) compared with control non-senescent BMEC monolayers (p ≤ 0.01). Inhibition of transcelluar permeability by Fillipin III (caveolae depletion) prevented increased transcellular albumin permeability in senescent mBMEC monolayers (p ≤ 0.05) confirming that "aging" process also affect barrier transcellular permeability (Fig. 1G).

As there is BBB leakage present in the aged brain, we evaluated the expression pattern of tight junction (TJ) proteins directly involved in controlling paracellular permeability. Claudin-5, a major BBB occlusion protein, and ZO-1 a major scaffolding protein showed fragmented and weaker staining in microvessels of old mice (18–22 months) and human brains compared to healthy young mice and "young" human brain samples (Fig. 2A). By Western blot, only claudin-5 showed a significant reduction in protein expression in aged mice (p < 0.001; Fig. 2B). However, as alterations in protein expression may only partially mirror changes in the TJ complex, the interaction between claudin-5 and ZO-1 was also examined. There was a dramatic reduction in the interaction between claudin-5 and ZO-1 in aged mice (Fig. 2C) that might represent a cause of the aging-associated BBB hyperpermeability.

3.2. Decline of Sirt1 in aging brain endothelial cells

To identify genes/markers of brain endothelial cell senescence, isolated human and mouse brain microvessels were subjected to gene array screen analysis. We analyzed 108 genes/markers of aging involved in genomic instability (telomere attrition, mitochondrial dysfunction, proteostasis, neurodegeneration and synaptic transmission, epigenetic alteration, DNA and RNA binding, inflammatory response, apoptosis, cellular senescence, cell cycle, cytoskeleton regulation oxidative stress and transcriptional regulators). In human brain microvessels, 61 genes were upregulated (greater than two-fold increase) while 12 genes were downregulated (greater than two-fold decrease) in the 'elderly' group. In mouse brain microvessels, 15 gene/markers of aging were upregulated and 6 downregulated in the aged group (Fig. 3A). The human microvessels showed most alterations in inflammation, mitochondrial dysfunction and epigenetic factors (total of 45 genes), while in mouse, most alterations were in inflammation and epigenetic factors (total of 17 genes). Among of the 10 genes that were altered in both mouse and human microvessels, Sirt1 showed same down regulation and magnitude of change in human (3.1-fold decrease) and mouse (2.7-fold decrease) aged microvessels. Real time PCR analysis confirmed the decreased Sirt1 mRNA expression in human (p < 0.05) and mouse (p < 0.01) (Fig. 3B). Sirt1 protein levels in human (Fig. 3C) and mouse (Fig. 3D) were also decreased, as was Sirt1 activity in mouse microvessels (p < 0.01; Fig. 3E).

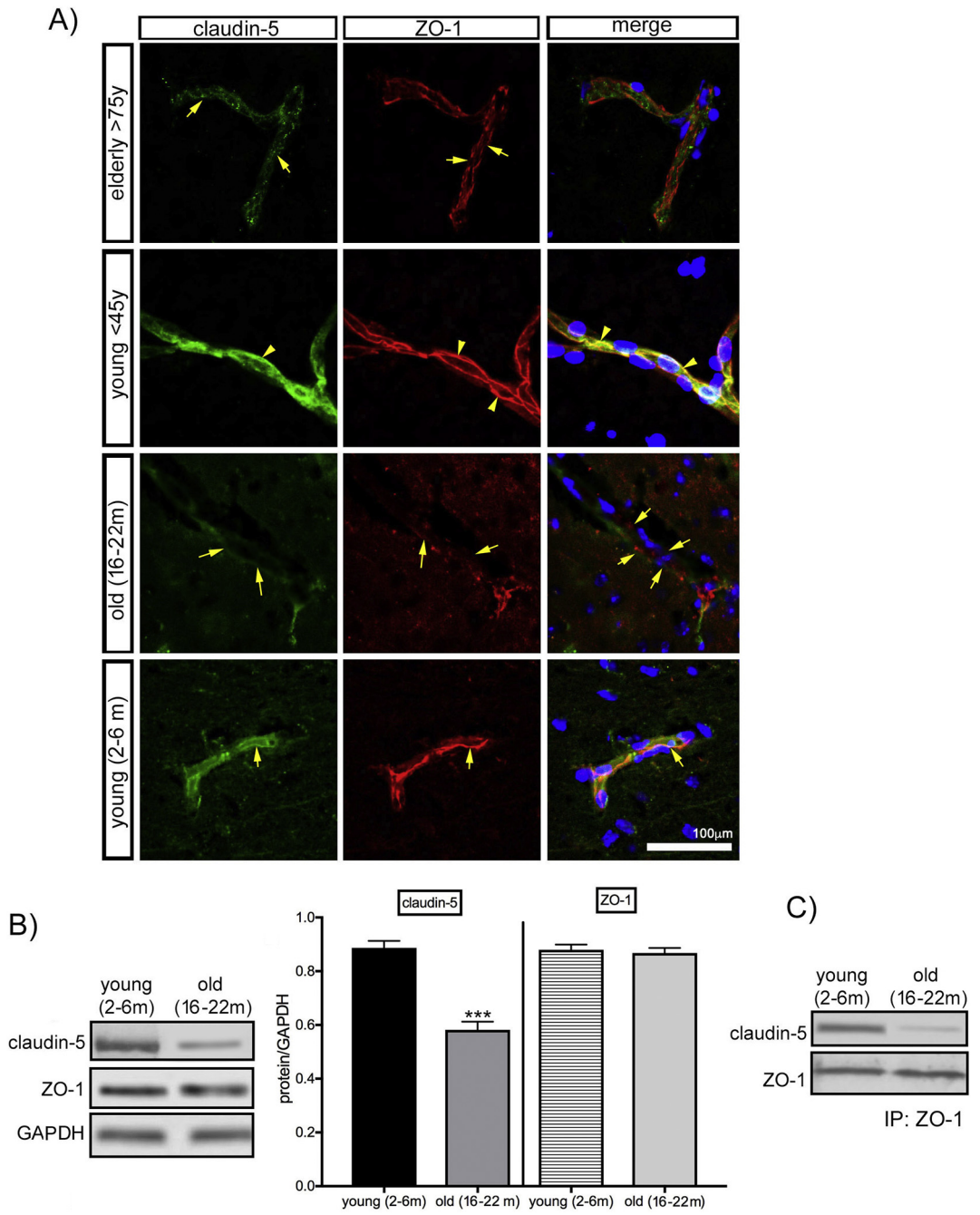

Fig. 2. A) Examples of immunofluorescence staining for claudin-5 (green) and ZO-1 (red) in an elderly human brain (> 75 years) and a young brain (< 45 years) as well as in old (20 months, group 16-22 m) and young (6 months, 2-6 m) mouse brain samples. Arrows and arrowhead indicates outline the microvessels. Notice the fragmented staining pattern for claudin-5 and ZO-1 in aged groups and decreased claudin-5 and ZO-1 expression in microvessels. Scale bar 100 μm. B) Western blot and semi-quantitative densitometric analysis of claudin-5 and ZO-1 protein expression in microvessels isolated from young (2-6 m) and old age (16-22 m) mice. Protein levels were normalized to GAPDH. Notice the decreased expression of claudin-5 while ZO-1 showed no alteration in total protein expression. Graph data represent means ± SD, n = 5; ***$p < 0.001$ compared to young age group. Western blotting image is one of five independent experiments. C) Immunoprecipitation (IP) and Western blot analysis of claudin-5 and ZO-1 interaction/co-localization in young (2–6 months) and old age (16–22 months) mice. Representative images of Western blot of three independent experiments. (For interpretation of the references to colour in this figure legend, the reader is referred to the web version of this article.)

3.3. Decline in Sirt1 is associated with alterations in BBB permeability in aging

The potential involvement of Sirt1 in regulating BBB permeability was assessed by modifying Sirt1 expression in brain endothelial cells via overexpression, global Sirt1 transgenic (Tg) mice, or conditional depletion of Sirt1 in brain endothelial cells, $Sirt^{Flox}/Cldn5^{icre}$ mice. An age-matched analysis (6 and 20 months) of BBB permeability to dextran 3 kDa in wild type and Sirt1 Tg mice revealed that the increase in BBB permeability present in aged wild type control was significantly reduced in SirtTg mice ($p < 0.001$; Fig. 4A). The Sirt1Tg mice had high Sirt1 expression in brain microvessels even at 20 months (Fig. 4C). Depleting Sirt1 specifically in brain endothelial cells ($Sirt1^{flox}Cldn5^{icre}$) resulted in increased BBB permeability to dextran 3 kDa ($p < 0.001$; Fig. 4B). Thus, both of these experiments indicate that Sirt1 regulates BBB permeability.

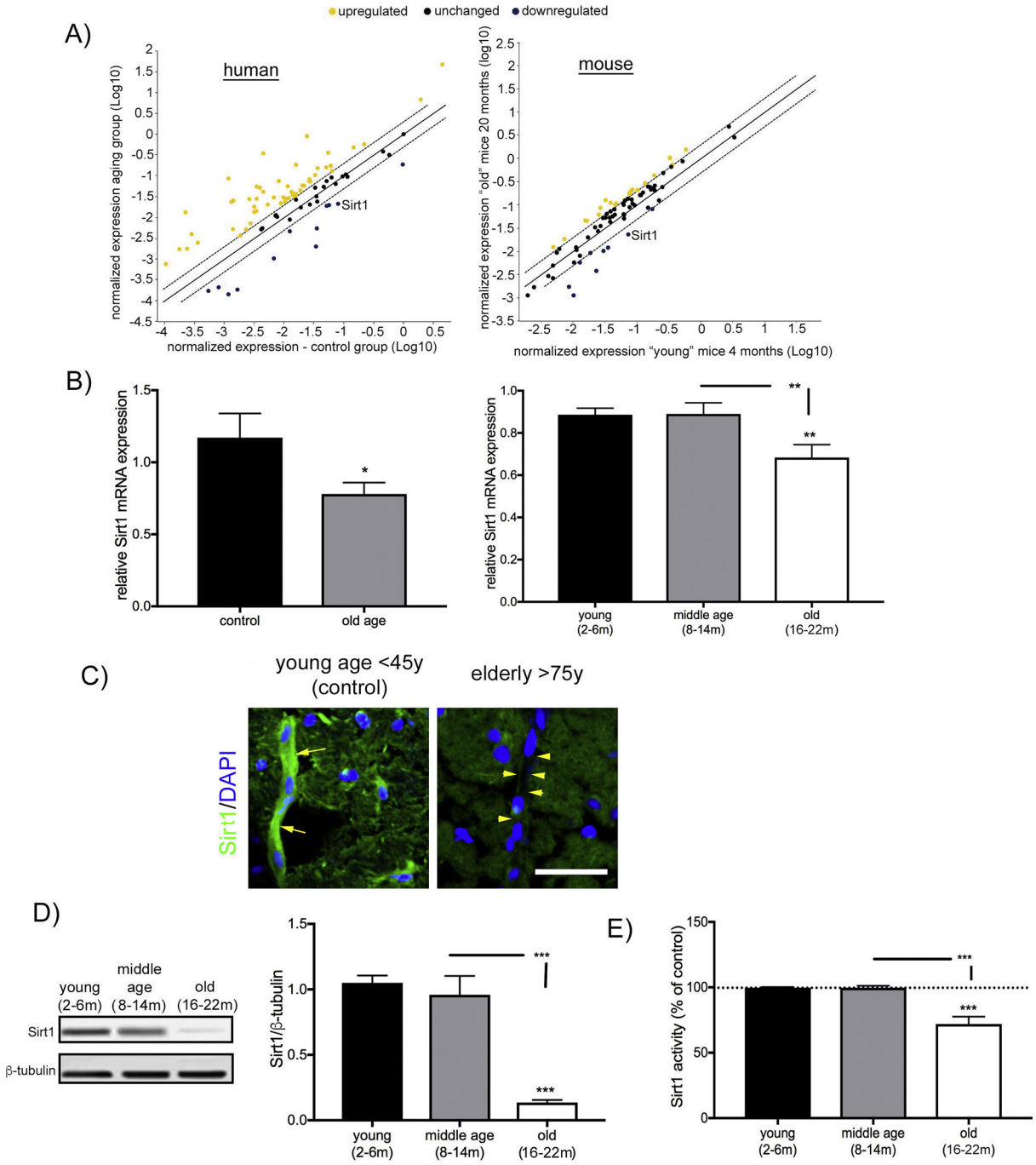

Fig. 3. A) Scatter plots showing the relationship between the mRNA expression of markers of aging in young (control group) and aged brain microvessels. Expression was normalized to panel of housekeeping genes included in plate. Left panel: human microvessels isolated from two cases of elderly (> 75 years old) brains compared to control young age (< 45 years old); Right panel: mouse brain microvessels isolated from aged (16–22 months) compared to young (2–6 months) mice. Changes in expression with aging were classified as upregulated or down regulated if there was a > 2 fold change. B) Real time RT-PCR analysis of Sirt1 mRNA expression in isolated human microvessels from young (< 45 years) and elderly (> 75 years) subjects as well young (2–6 months), middle (8–14 months) and old (16–22 months) mice. mRNA levels were normalized to GAPDH. Notice there was a decline of Sirt1 expression in the aged group in both humans and mice. Graph data represent means ± SD, n = 3; *p < 0.05 and **p < 0.01 compared with young as well middle-age groups. C) Example of immunofluorescence staining for Sirt1 (green) in a young human brain (< 45 years; control) and an elderly brain sample (> 75 years). Arrows and arrowhead indicates line of the microvessels and demonstrate the decreased microvascular Sirt1 expression. Scale bar 50 μm. D) Western blot analysis of Sirt1 protein expression in isolated brain microvessels from young (2–6 months), middle (8–14 months) and old (16–22 months) mice. Notice the decreased expression of Sirt1 in the old age group. E) Sirt1 activity was measured in isolated microvessels in all the aging groups. Graph represents means ± SD, n = 3; comparing with young age group. (For interpretation of the references to colour in this figure legend, the reader is referred to the web version of this article.)

Similar to the in vivo data, reducing Sirt1 expression in brain endothelial cells by transfection with Sirt1 siRNA increased barrier permeability (Fig. 4C). Monolayers of mBMEC overexpressing Sirt1 (cells isolated from Sirt1Tg mice) had a very low permeability to the tracer FITC-inulin (Fig. 4C). Senescence in mBMEC, induced either by continuous passage or oxidative stress (H_2O_2 treatment), also reduced Sirt1 protein expression and activity (Fig. 4D). Stable and increased expression of Sirt1 in brain endothelial cells (Sirt1Tg BMEC) showed

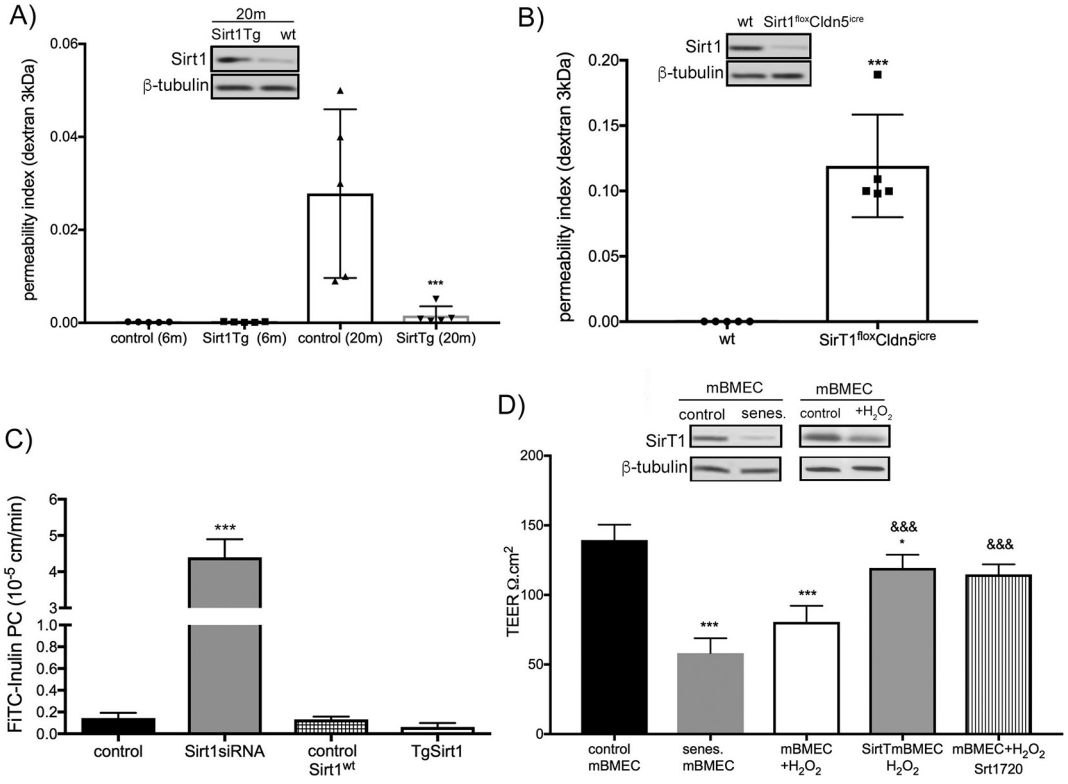

Fig. 4. A) Permeability index (blood to brain flux) for dextran 3 kDa evaluated in whole brain samples of wild type (wt; control) and Sirt1 transgenic (Sirt1Tg) mice at 6 and 20 months. Notice the increased permeability for dextran 3 kDa in aged wt group at 20 months while Sirt1 transgenic mice (SirtTg) had a low permeability at the same age. Graph data represent means ± SD, n = 5; ***p < 0.001 control vs. SirtTg at 20 months. Representative Western blot of Sirt1 expression in brain microvessels in Sirt1Tg and wt mice at 20 months. B) Permeability index for tracer dextran 3 kDa measured in conditional knockout ($Sirt1^{flox}Cldn5^{icre}$) mice demonstrated that altering Sirt1 expression in brain endothelial cells increased BBB permeability. Graph data represent means ± SD, n = 5; ***p < 0.001 comparing control (wt) and conditional knockout ($Sirt1^{flox}Cldn5^{icre}$) mice. Western blot shows the impact of the conditional knockout on microvessel Sirt1. C) Altering Sirt1 expression in brain endothelial cells affects the permeability of mBMEC monolayer in vitro. Sirt1 depletion was achieved by knocking down Sirt1 (transfection with Sirt1 siRNA) and this increased inulin permeability coefficient (PC). Overexpression of Sirt1 (mBMEC from Sirt1Tg mice) showed stable and impermeable mBMEC monolayer for inulin. Graph data represent means ± SD, $n = 5$. D) TEER measurements in mBMEC monolayers produced from control or senescent mBMEC produced by passage (senes. mBMEC), or treatment with 100 μM H_2O_2 (mBMEC + H_2O_2). Senescence reduced the TEERs of mBMEC monolayers. mBMEC prepared from Sirt1 transgenic (Tg) mice (Sirt-mBMEC) or treated with the Sirt1 agonist Srt1720 were both protected against the effects of H_2O_2. The graph shows means ± SD, n = 3; *p < 0.05, ***p < 0.001 comparing control and senescent mBMEC and SirtTg monolayers; $^{\&\&\&}p < 0.001$ comparing senescence mBMEC with SirtTg-mBMEC and mBMEC treated with Srt1720.

resistance to senescence-induced reductions in brain endothelial barrier integrity (Fig. 4D). Likewise, compensating for senescence-induced reduced Sirt1 expression by increasing Sirt1 activity with a Sirt1 agonist, SRT1720, also reduced brain endothelial barrier permeability in senescent BMEC (Fig. 4D).

Sirt1-mediated effects on BBB permeability were associated with altered TJ protein expression. Expression of the major brain endothelial TJ protein claudin-5 was decreased with the decline in Sirt1 in aging mice as well as in mice with depleted brain endothelial cell Sirt1 (Fig. 5A and B). Moreover, overexpression of Sirt1 (Sirt1 Tg mice) and an absence of the decline during aging affect claudin-5 expression protein and mRNA in brain endothelial cells. (Fig. 5A, B). Modifying Sirt1 in brain endothelial cells did not affect the ZO-1 expression (Fig. 5A). The cellular Sirt1 effects on the brain endothelial permeability and TJ complex stability were further assessed in vitro. Morphologically, in contrast to the continuous staining of claudin-5 and ZO-1 present in controls, in senescent cells there was more fragmented claudin-5 staining and a comb-like pattern of ZO-1 staining with loss of interaction between claudin-5 and ZO-1 evaluated by dual link assay (Fig. 5C and D). Similarly, depleting Sirt1, by transfection with Sirt1 siRNA, caused a very similar pattern, fragmented claudin-5, comb-like ZO-1 structures with loss of interaction between claudin-5 and ZO-1 (Fig. 5C).

Rescue of Sirt1 in senescent cells affected both permeability and TJ complex stability (Fig. 5C and D). Treating BMEC with the Sirt1 agonist (Srt1720) only partially restored claudin-5 protein expression but more markedly affected claudin-5 and ZO-1 interaction/colocalization at the cell border, affecting brain endothelial barrier permeability (Fig. 5D). This suggests that Sirt1 plays a key role in regulating barrier stability probably through modifying protein expression and protein-protein interactions in the TJ complex.

4. Discussion

The present study revealed new insights into morphological and functional alterations at the BBB during aging. In particular, our results highlighted that: 1) aging/ senescence in brain endothelial cells directly affects barrier property and claudin-5 mRNA and protein expression, 2) a key mediator of the aging process and aging related BBB hyperpermeability is a reduction in Sirt1, 3) Sirt1 is involved in regulating claudin-5 and its interactions in the TJ complex, 4) rescuing Sirt1 expression or activity in the aged BBB can protect barrier integrity. These finding are discussed below.

Aging is a complex and multifactorial process, manifested as progressive loss of physiological integrity and function. Healthy aging is associated with a series of morphological, metabolic and epigenetic alterations, limiting regeneration and plasticity, and making cells/ tissue vulnerable to diseases, infection and stress. In general, barrier

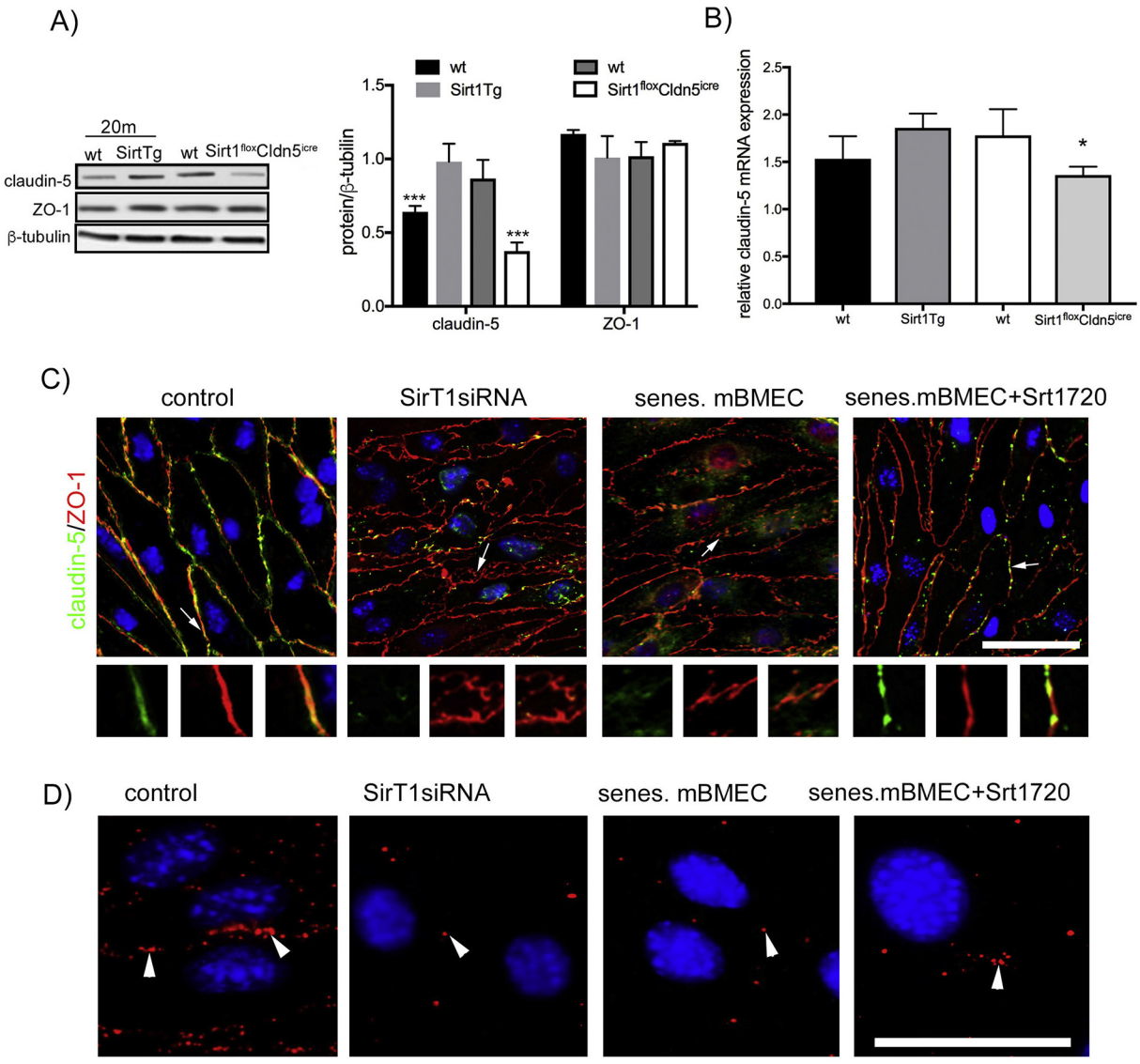

Fig. 5. A) Representative Western blot of claudin-5 and ZO-1 expression in brain microvessels in Sirt1 transgenic mice (Sirt1Tg) and wildtype (wt) controls, both aged 20 months, and conditional Sirt1 brain endothelial knockout mice ($Sirt1^{flox}Cldn5^{icre}$) and corresponding wt controls. Graph represents semiquantitative densitometric analysis of claudin-5 expression in Sirt1Tg and wt mice, as well Sirt1 brain endothelial knockout mice ($Sirt1^{flox}Cldn5^{icre}$) and wt controls. Value are means ± SD, n = 3, $p < 0.001$. B) Real time RT-PCR analysis of claudin-5 mRNA expression in mouse blood vessels isolated from Sirt1Tg mice and corresponding controls (aged 20 months), and conditional Sirt1 knockout mice ($Sirt1^{flox}Cldn5^{icre}$) and corresponding controls. mRNA levels were normalized to GAPDH. Notice there was decline of claudin-5 expression in conditional Sirt1 knockout mice. Graph represents means ± SD, n = 3; *$p < 0.05$ compared with corresponding control (wt) group. C) Immunofluorescence staining for claudin-5 (green) and ZO-1 (red) in control, Sirt1 knockdown mBMEC (Sirt1 siRNA), senescent (senes.) mBMEC and in condition of rescue Sirt1 in senescent mBMEC (senes.mBMEC + Srt1720). Arrow and zoom images (box) indicate localization of ZO-1 and claudin-5 on the cell. Scale bar 50 μm. D) Claudin-5/ZO-1 interaction analyzed by proximity ligation assay (PLA) in control (non-exposed cells), Sirt1 knockdown cells (Sirt1 siRNA), senescent mBMEC (senes. mBMEC) and senescent mBMEC treated with Sirt1 agonist (senes.mBMEC + Srt1720). mBMEC monolayers were PLA labeled using claudin-5 and ZO-1 antibodies. Arrowhead indicates points of claudin-5/ZO-1 interaction. Scale bar 20 μm. (For interpretation of the references to colour in this figure legend, the reader is referred to the web version of this article.)

tissues in undergo age-dependent remodeling manifested as changes in functional status including increased permeability (Delaney and Campbell, 2017; Parrish, 2017). Age-related increases in BBB permeability have been widely report in recent years. In particular, human studies based on magnetic resonance imaging (MRI), have shown compromised and leaky BBB in elderly patients with neurodegenerative diseases, cardiovascular and cerebrovascular pathology, but also in conditions when other age-related risk-factors (hypertension, high cholesterol, inflammation) are not present (Grinberg and Thal, 2010; Kaur et al., 2011; Rouhl et al., 2012; Simpson et al., 2010). Similarly, in experimental studies, an aged compromised BBB has been reported associated with different model diseases (e.g. in Alzheimer's disease models), predominantly in area affected with ongoing pathology (e.g. cortex or hippocampus) (Bell and Zlokovic, 2009; Montagne et al., 2015). However, senescence induced-BBB hyperpermeability is also present in senescence-accelerated mice with no ongoing brain pathological process, showing that BBB permeability could be induced by ongoing senescence processes at the BBB (Banks et al., 2000; Banks et al., 2007; Zhang et al., 2013). In the current study, we report that "healthy aging processes" affect barrier stability resulting in a progressive size-dependent BBB hyperpermeability in old mice. This age-associated BBB permeability appeared global, although we cannot exclude that differences exist in certain brain regions, cortex vs cerebellum, or cortex vs basal ganglia, reported in several studies (Elahy

et al., 2015; Lee et al., 2012; Montagne et al., 2015).

The degree of BBB hyperpermeability is closely associated with the magnitude of TJ changes, varying from complete loss of some TJ proteins (e.g. claudin-5 and occludin) and uncontrolled increases in vascular permeability (BBB breakdown), to morphologically fragmented or "difficult to detect" alterations in TJ proteins that can cause small but persistent leaks with excessive perivascular build-up of fluid (BBB leakage) (Stamatovic et al., 2016). At the aging BBB, alterations in the TJ proteins claudin-5, ZO-1 and occludin have been reported with fragmented staining and various degrees of total protein loss (Elahy et al., 2015; Kaur et al., 2011; Lee et al., 2012; Yang et al., 2018). A key event for a compromised BBB is an alteration in claudin-5, a major occlusion protein for brain endothelial barrier. It has been reported that claudin-5 protein expression is changed/reduced in aging brain endothelial cells (Elahy et al., 2015; Yamazaki et al., 2016; Yang et al., 2018). In agreement, the current study showed that claudin-5 mRNA and protein slowly decline over the lifespan in mice and similarly in human brain microvessels. This decline is reflected in claudin-5 incorporation into the TJ complex and claudin-5 strands. Senescent brain endothelial cells showed more fragmented features with gap formation between cells. In addition to alterations at the total protein level, an analysis of protein-protein interaction revealed that claudin-5 loses an essential interaction with ZO-1. Claudin-5/ZO-1 interaction is pivotal for the localization of claudin-5 in the TJ complex and for establishing homophilic transcellular-adhesive interactions (Piontek et al., 2011). Reduced protein interaction with ZO-1 weakens claudin-5 trans-interactions, which represents a solid ground for generating gaps in claudin-5 strands. Future studies should examine the dynamics of claudin-5 in the TJ complex as well remodeling of protein-protein interaction in the aging barrier.

BBB hyperpermeability may be triggered a variety of microenvironmental factors (inflammatory mediators, growth factors), as well as endothelial intrinsic factors (e.g. vascular injury, altered oxidative metabolism) (Kelly et al., 2009; Lee et al., 2012; Rouhl et al., 2012). Numerous studies have pinpointed that remodeling of the neurovascular unit has a critical role in BBB hyperpermeability in aging (Heye et al., 2014; Kaur et al., 2011). Astrocytes as well pericytes are altered in aging, and particularly in aging-associated neurodegenerative disease, affecting BBB permeability (Bell and Zlokovic, 2009; Halliday et al., 2016). Their effects involve the secretion of proinflammatory mediators and angiogenic factors as well alterations in the extracellular matrix, which might modulate ongoing perivascular processes (e.g. inflammation) and alter BBB permeability and junction protein expression (Elahy et al., 2015; Lee et al., 2012).

Brain endothelial cells also undergo senescence, displaying morphological (degenerative and focal necrotic changes) and metabolic (decreased mitochondrial content) changes as well alterations in permeability (increased pinocytotic vesicles, loss of TJs) and thickening of the basal lamina (Farrall and Wardlaw, 2009; Grinberg and Thal, 2010). A variety of factors could be involved including, but not limited to, oxidative stress, reduced nitric oxide, proinflammatory cytokines (IL6, IL1β, chemokines), matrix metalloproteinases as well epigenetic factors, such as Sirt1 (Brown and Thore, 2011; Delaney and Campbell, 2017; Elahy et al., 2015; Lee et al., 2012). All of these factors may be targets but also effectors of the senescence process. Our screening gene analysis identified that senescent brain endothelial cells in human and mouse microvessels have similar gene profiles including a significant downregulation in Sirt1.

Sirt1 is recognized as a key regulator of vascular endothelial homeostasis, controlling angiogenesis, endothelial senescence and dysfunction. As an anti-aging molecule, Sirt1 targets several cell-processes including apoptosis and longevity (by regulating FoxO3a), bioavailability and oxidative stress (by regulating NOS3) (Imai and Guarente, 2014; Mouchiroud et al., 2013). It is highly expressed in brain tissue compared to other organs. It is particularly expressed in neurons, where its distribution depends on brain region, and in cerebral arteries and smooth muscle cells (Li and Wang, 2017; Wan et al., 2018; Zhou et al., 2017). Several recent studies indicate a beneficial effect of Sirt1 in neurodegenerative disease as well neuronal injury after cerebral ischemia (Chen et al., 2018; Hattori et al., 2014; Min et al., 2018; Zhou et al., 2017). Regarding the BBB, a beneficial effect of Sirt1 was indicated by reduced brain edema in subarachnoid hemorrhage and in the protection of BBB integrity during ischemic injury (Chen et al., 2018; Zhou et al., 2017). The effects of Sirt1 were proposed to be anti-apoptotic by targeting p53 deacetylation, anti-oxidative in interaction with Sirt3, and anti-inflammatory by reducing MMP9, Cox-2 expression and NFκB activity although a direct effect of Sirt1 on TJ protein expression was not indicated (Chen et al., 2018; Mouchiroud et al., 2013; Yang et al., 2012; Zhou et al., 2017).

Sirt1 effect on aging process is directly depending on the Sirt1 expression and activity level in cells. Decline in Sirt1 expression/activity in aging was reported to be mediated via transcriptional, post-translational modification and miRNAs (Buler et al., 2016). In age-dependent transcriptional Sirt1 modification, repression of C/EBPβ-HDAC1 complex, FOXO1, p53, BMAL1 are indicated (Jin et al., 2011; Xiong et al., 2011; Zhou et al., 2014). Moreover Sirt1 gene polymorphism is implicated in alteration of Sirt1 expression during aging and in accelerated aging (Kilic et al., 2015). miRNA, particularly, miR34, miR9, miR132, are important transcriptional regulators of Sirt1 expression in aging by direct binding to the Sirt1 promoter or indirectly, by regulating deacetylation and activity of p53 (Nemoto et al., 2004; Qi et al., 2015; Zhang et al., 2014). At the post-translational level, phosphorylation, ubiquitination, sumylation, carbonilation, S-gluthionylation and methylation could control Sirt1 level activity, nuclear localization, and its response on oxidative stress and DNA damage (Caito et al., 2010; Peng et al., 2015; Yang et al., 2007). Aging and cell senescence is directly associated with increased and accumulated oxidative stress and inflammatory mediators (e.g. NFκB), and these processes play critical roles in age-associated decline of Sirt1 expression and activity (Bagul et al., 2015). However, there is complex and bidirectional interplay between Sirt1 and factors/process that regulate its expression/activity leading to the hypothesis of the existence of a feedback mechanism where oxidative stress, inflammatory mediators and Sirt1 are in a close "vicious circle", triggering and progression cell senescence (Buler et al., 2016).

Our results demonstrate that age-dependent modification of Sirt1 expression, overexpression or knockdown, affects claudin-5 expression at the mRNA and protein levels and consequently the BBB integrity. Sirt1 has been reported to regulate TJ protein expression in other tissues. Sirt1, via deacetylation of transcriptional factor Klf4, activated claudin-5 transcription in ovarian cancer cells (Zhang et al., 2018). Transcriptional regulation of claudin-1 by Sirt1 was reported in lung and kidney epithelial cells, where Sirt1 causes direct methylation of CpG sites in the claudin-1 promoter (Hasegawa et al., 2013). Similar effects have been reported for ZO-1 in gut (Bein et al., 2017). Other signaling pathways include the activation of AMPK signaling by Sirt1 to indirectly regulate oxidative metabolism in cells and BBB stability (Zhao et al., 2017). Thus, Sirt1 may directly or indirectly regulate claudin-5 expression at the transcriptional and translation level and potentially other junction proteins, consequently affecting BBB permeability. Thus, it is perhaps not surprising that age-associated reductions in Sirt1 expression/ activity are correlated with BBB hyperpermeability. Aging reduces Sirt1 activity and overtime decreases Sirt1 expression in brain endothelial cells that further affect cell metabolism and could also cause age-associated epigenetic modification. Sirt1 regulation of BBB permeability could, thus, involve transcriptional modification of TJ proteins synthesis (e.g. decline in deacetylation of transcriptional factors NFκB or Klf4) or signaling pathways regulating the oxidative stress and inflammatory response of brain endothelial cells and consequently modification of TJ proteins (e.g. claudin-5) and their protein-protein interaction. As the aging process results in a progressive decline in BBB integrity, the slow decline in Sirt1 may impact

an increasing number of signaling molecules and pathways regulating BBB permeability. Thus, modifying the expression/ activity of Sirt1 in endothelial cells could be promising target for reducing aging-associated BBB hyperpermeability. Furthermore, the effect of Sirt1 decline in aging on BBB permeability is not limited to brain endothelial cells. Aging processes also affect other cells in the neurovascular unit, astrocytes, pericytes, perivascular macrophages and neurons. Sirt1 decline in astrocytes is associated with increased gliosis and production of proinflammatory cytokines directing the inflammatory response in neurodegenerative disorders, Alzheimer disease, and HIV brain infection (Hu et al., 2017; Li et al., 2017; Scuderi et al., 2014). Similarly, pericyte responses to HIV infection and increased senescence are associated with decreases in Sirt1 expression (Castro et al., 2016). Thus, it is not surprising that the stability of the senescent BBB in vitro (brain endothelial cell-astrocyte co-culture) was impaired. Astrocytes and probably pericytes may indirectly via triggering or supporting inflammation or oxidative damage, affect and further amplify ongoing barrier impairment.

In summary, a compromised BBB in aging plays an important role in disease pathophysiology due to leakage and accumulation of blood components in brain parenchyma and vessel walls which may cause further age-related brain pathology and is associated with increased incidence of stroke (Cai et al., 2017; Kaur et al., 2011). Sirt1, as one upstream regulator of several ongoing processes in aging cells and the BBB could represent a good target to prevent or delay the aging process at the BBB. Enhancing Sirt1 expression/activity could be an ultimate goal in preventing aging BBB pathology.

Supplementary data to this article can be found online at https://doi.org/10.1016/j.nbd.2018.09.006.

Acknowledgment

This work was supported by Public Health Service grants RF1AG057928 and RFA057928 from National Institute of Aging (NIA) United States (A.V.A), 1-16-IBS-008 from American Diabetes Association and NS098211 from the National Institute of Neurological Disorders (S.M.S). Tissue specimens were obtained from the Human Brain and Spinal Fluid Resource Center (West Los Angeles Healthcare Center, Los Angeles, USA) and Mount Sinai NBTR (New York, USA). The confocal microscopy work was performed in the Microscopy and Image-analysis Laboratory (MIL) at the University of Michigan, Department of Cell & Developmental Biology.

References

Abbott, N.J., et al., 2010. Structure and function of the blood-brain barrier. Neurobiol. Dis. 37, 13–25.
Bagul, P.K., et al., 2015. Resveratrol ameliorates cardiac oxidative stress in diabetes through deacetylation of NFkB-p65 and histone 3. J. Nutr. Biochem. 26, 1298–1307.
Banks, W.A., et al., 2000. Permeability of the blood-brain barrier to albumin and insulin in the young and aged SAMP8 mouse. J. Gerontol. A Biol. Sci. Med. Sci. 55, B601–B606.
Banks, W.A., et al., 2007. Anti-amyloid beta protein antibody passage across the blood-brain barrier in the SAMP8 mouse model of Alzheimer's disease: an age-related selective uptake with reversal of learning impairment. Exp. Neurol. 206, 248–256.
Bein, A., et al., 2017. Intestinal tight junctions are severely altered in NEC preterm neonates. Pediatr. Neonatol. https://doi.org/10.1016/j.pedneo.2017.11.018. (Dec 7. pii: S1875-9572(17)30025-6).
Bell, R.D., Zlokovic, B.V., 2009. Neurovascular mechanisms and blood-brain barrier disorder in Alzheimer's disease. Acta Neuropathol. 118, 103–113.
Brown, W.R., Thore, C.R., 2011. Review: cerebral microvascular pathology in ageing and neurodegeneration. Neuropathol. Appl. Neurobiol. 37, 56–74.
Buler, M., et al., 2016. Who watches the watchmen? Regulation of the expression and activity of sirtuins. FASEB J. 30, 3942–3960.
Cai, W., et al., 2017. Dysfunction of the neurovascular unit in ischemic stroke and neurodegenerative diseases: an aging effect. Ageing Res. Rev. 34, 77–87.
Caito, S., et al., 2010. SIRT1 is a redox-sensitive deacetylase that is post-translationally modified by oxidants and carbonyl stress. FASEB J. 24, 3145–3159.
Castro, V., et al., 2016. Occludin controls HIV transcription in brain pericytes via regulation of SIRT-1 activation. FASEB J. 30, 1234–1246.
Chang, H.C., Guarente, L., 2014. SIRT1 and other sirtuins in metabolism. Trends Endocrinol. Metab. 25, 138–145.
Chang, E., Harley, C.B., 1995. Telomere length and replicative aging in human vascular tissues. Proc. Natl. Acad. Sci. U. S. A. 92, 11190–11194.
Chen, Q., et al., 1995. Oxidative DNA damage and senescence of human diploid fibroblast cells. Proc. Natl. Acad. Sci. U. S. A. 92, 4337–4341.
Chen, Y.X., et al., 2015. The Sirt1 activator SRT1720 attenuates angiotensin II-induced atherosclerosis in apoE(−)/(−) mice through inhibiting vascular inflammatory response. Biochem. Biophys. Res. Commun. 465, 732–738.
Chen, T., et al., 2018. Sirt1-Sirt3 axis regulates human blood-brain barrier permeability in response to ischemia. Redox Biol. 14, 229–236.
Delaney, C., Campbell, M., 2017. The blood brain barrier: Insights from development and ageing. Tissue Barriers. 5, e1373897.
Dierick, J.F., et al., 2002. Identification of 30 protein species involved in replicative senescence and stress-induced premature senescence. FEBS Lett. 531, 499–504.
Dimri, G.P., et al., 1995. A biomarker that identifies senescent human cells in culture and in aging skin in vivo. Proc. Natl. Acad. Sci. U. S. A. 92, 9363–9367.
Ding, M., et al., 2015. SIRT1 protects against myocardial ischemia-reperfusion injury via activating eNOS in diabetic rats. Cardiovasc. Diabetol. 14, 143.
Elahy, M., et al., 2015. Blood-brain barrier dysfunction developed during normal aging is associated with inflammation and loss of tight junctions but not with leukocyte recruitment. Immun. Ageing 12, 2.
Farrall, A.J., Wardlaw, J.M., 2009. Blood-brain barrier: ageing and microvascular disease–systematic review and meta-analysis. Neurobiol. Aging 30, 337–352.
Gonzalez-Mariscal, L., et al., 2003. Tight junction proteins. Prog. Biophys. Mol. Biol. 81, 1–44.
Gorelick, P.B., et al., 2011. Vascular contributions to cognitive impairment and dementia: a statement for healthcare professionals from the american heart association/american stroke association. Stroke 42, 2672–2713.
Grinberg, L.T., Thal, D.R., 2010. Vascular pathology in the aged human brain. Acta Neuropathol. 119, 277–290.
Guerriero, F., et al., 2017. Neuroinflammation, immune system and Alzheimer disease: searching for the missing link. Aging Clin. Exp. Res. 29, 821–831.
Halliday, M.R., et al., 2016. Accelerated pericyte degeneration and blood-brain barrier breakdown in apolipoprotein E4 carriers with Alzheimer's disease. J. Cereb. Blood Flow Metab. 36, 216–227.
Hasegawa, K., et al., 2013. Renal tubular Sirt1 attenuates diabetic albuminuria by epigenetically suppressing Claudin-1 overexpression in podocytes. Nat. Med. 19, 1496–1504.
Hattori, Y., et al., 2014. Silent information regulator 2 homolog 1 counters cerebral hypoperfusion injury by deacetylating endothelial nitric oxide synthase. Stroke 45, 3403–3411.
Heye, A.K., et al., 2014. Assessment of blood-brain barrier disruption using dynamic contrast-enhanced MRI. A systematic review. Neuroimage Clin. 6, 262–274.
Hori, Y.S., et al., 2013. Regulation of FOXOs and p53 by SIRT1 modulators under oxidative stress. PLoS One 8, e73875.
Hu, G., et al., 2017. Tat-mediated induction of miRs-34a & -138 promotes astrocytic activation via downregulation of SIRT1: implications for aging in HAND. J. NeuroImmune Pharmacol. 12, 420–432.
Imai, S., Guarente, L., 2014. NAD+ and sirtuins in aging and disease. Trends Cell Biol. 24, 464–471.
Jin, J., et al., 2011. The reduction of SIRT1 in livers of old mice leads to impaired body homeostasis and to inhibition of liver proliferation. Hepatology 54, 989–998.
Kauppinen, A., et al., 2013. Antagonistic crosstalk between NF-kappaB and SIRT1 in the regulation of inflammation and metabolic disorders. Cell. Signal. 25, 1939–1948.
Kaur, J., et al., 2011. Quantitative MRI reveals the elderly ischemic brain is susceptible to increased early blood-brain barrier permeability following tissue plasminogen activator related to claudin 5 and occludin disassembly. J. Cereb. Blood Flow Metab. 31, 1874–1885.
Kazakoff, P.W., et al., 1995. An in vitro model for endothelial permeability: assessment of monolayer integrity. In Vitro Cell Dev. Biol. Anim. 31, 846–852.
Kelly, K.A., et al., 2009. NOX2 inhibition with apocynin worsens stroke outcome in aged rats. Brain Res. 1292, 165–172.
Kilic, U., et al., 2015. A remarkable age-related increase in SIRT1 protein expression against oxidative stress in elderly: SIRT1 gene variants and longevity in human. PLoS One 10, e0117954.
Koronowski, K.B., et al., 2017. Neuronal SIRT1 (Silent Information Regulator 2 Homologue 1) regulates glycolysis and mediates resveratrol-induced ischemic tTolerance. Stroke 48, 3117–3125.
Lee, M.Y., et al., 2010. Senescence of cultured porcine coronary arterial endothelial cells is associated with accelerated oxidative stress and activation of NFkB. J. Vasc. Res. 47, 287–298.
Lee, P., et al., 2012. Effects of aging on blood brain barrier and matrix metalloproteases following controlled cortical impact in mice. Exp. Neurol. 234, 50–61.
Li, H., Wang, R., 2017. Blocking SIRT1 inhibits cell proliferation and promotes aging through the PI3K/AKT pathway. Life Sci. 190, 84–90.
Li, Y., et al., 2014. Novel role of silent information regulator 1 in acute endothelial cell oxidative stress injury. Biochim. Biophys. Acta 1842, 2246–2256.
Li, D., et al., 2017. Interactions between Sirt1 and MAPKs regulate astrocyte activation induced by brain injury in vitro and in vivo. J. Neuroinflammation 14, 67.
Min, S.W., et al., 2018. SIRT1 Deacetylates Tau and Reduces Pathogenic Tau Spread in a Mouse Model of Tauopathy. J. Neurosci. 38, 3680–3688.
Montagne, A., et al., 2015. Blood-brain barrier breakdown in the aging human hippocampus. Neuron 85, 296–302.
Mouchiroud, L., et al., 2013. The NAD(+)/sirtuin pathway modulates longevity through activation of mitochondrial UPR and FOXO signaling. Cell 154, 430–441.
Nemoto, S., et al., 2004. Nutrient availability regulates SIRT1 through a forkhead-dependent pathway. Science 306, 2105–2108.

Pantoni, L., 2010. Cerebral small vessel disease: from pathogenesis and clinical characteristics to therapeutic challenges. Lancet Neurol. 9, 689–701.
Parrish, A.R., 2017. The impact of aging on epithelial barriers. Tissue Barriers. 5, e1343172.
Peng, L., et al., 2015. Ubiquitinated sirtuin 1 (SIRT1) function is modulated during DNA damage-induced cell death and survival. J. Biol. Chem. 290, 8904–8912.
Piontek, J., et al., 2011. Elucidating the principles of the molecular organization of heteropolymeric tight junction strands. Cell. Mol. Life Sci. 68, 3903–3918.
Qi, F., et al., 2015. MiR-9a-5p regulates proliferation and migration of hepatic stellate cells under pressure through inhibition of Sirt1. World J. Gastroenterol. 21, 9900–9915.
Richardson, K., et al., 2012. The neuropathology of vascular disease in the Medical Research Council Cognitive Function and Ageing Study (MRC CFAS). Curr. Alzheimer Res. 9, 687–696.
Rouhl, R.P., et al., 2012. Vascular inflammation in cerebral small vessel disease. Neurobiol. Aging 33, 1800–1806.
Scuderi, C., et al., 2014. Sirtuin modulators control reactive gliosis in an in vitro model of Alzheimer's disease. Front. Pharmacol. 5, 89.
Simpson, J.E., et al., 2010. Alterations of the blood-brain barrier in cerebral white matter lesions in the ageing brain. Neurosci. Lett. 486, 246–251.
Sladojevic, N., et al., 2014. Inhibition of junctional adhesion molecule-A/LFA interaction attenuates leukocyte trafficking and inflammation in brain ischemia/reperfusion injury. Neurobiol. Dis. 67, 57–70.
Stamatovic, S.M., et al., 2003. Potential role of MCP-1 in endothelial cell tight junction 'opening': signaling via Rho and Rho kinase. J. Cell Sci. 116, 4615–4628.
Stamatovic, S.M., et al., 2006. Protein kinase Calpha-RhoA cross-talk in CCL2-induced alterations in brain endothelial permeability. J. Biol. Chem. 281, 8379–8388.
Stamatovic, S.M., et al., 2016. Junctional proteins of the blood-brain barrier: New insights into function and dysfunction. Tissue Barriers. 4, e1154641.
Tajbakhsh, N., Sokoya, E.M., 2012. Regulation of cerebral vascular function by sirtuin 1. Microcirculation 19, 336–342.
Ueno, M., et al., 1993. Age-related changes in barrier function in mouse brain I. Accelerated age-related increase of brain transfer of serum albumin in accelerated senescence prone SAM-P/8 mice with deficits in learning and memory. Arch. Gerontol. Geriatr. 16, 233–248.
Wan, W., et al., 2018. PDGFR-beta modulates vascular smooth muscle cell phenotype via IRF-9/SIRT-1/NF-kappaB pathway in subarachnoid hemorrhage rats. J. Cereb. Blood Flow Metab. https://doi.org/10.1177/0271678X18760954. (Feb 26:271678X18760954; Epub ahead of print).
Wardlaw, J.M., 2008. What is a lacune? Stroke 39, 2921–2922.
Wardlaw, J.M., et al., 2008. Changes in background blood-brain barrier integrity between lacunar and cortical ischemic stroke subtypes. Stroke 39, 1327–1332.
Xiong, S., et al., 2011. FoxO1 mediates an autofeedback loop regulating SIRT1 expression. J. Biol. Chem. 286, 5289–5299.
Yamazaki, Y., et al., 2016. Vascular cell senescence contributes to blood-brain barrier breakdown. Stroke 47, 1068–1077.
Yang, Y., et al., 2007. SIRT1 sumoylation regulates its deacetylase activity and cellular response to genotoxic stress. Nat. Cell Biol. 9, 1253–1262.
Yang, L., et al., 2012. SIRT1 regulates CD40 expression induced by TNF-alpha via NF-kB pathway in endothelial cells. Cell. Physiol. Biochem. 30, 1287–1298.
Yang, Y., et al., 2018. Vascular tight junction disruption and angiogenesis in spontaneously hypertensive rat with neuroinflammatory white matter injury. Neurobiol. Dis. 114, 95–110.
Zhang, X., et al., 2013. Age-related alteration in cerebral blood flow and energy failure is correlated with cognitive impairment in the senescence-accelerated prone mouse strain 8 (SAMP8). Neurol. Sci. 34, 1917–1924.
Zhang, L., et al., 2014. MiR-132 inhibits expression of SIRT1 and induces pro-inflammatory processes of vascular endothelial inflammation through blockade of the SREBP-1c metabolic pathway. Cardiovasc. Drugs Ther. 28, 303–311.
Zhang, X., et al., 2018. SIRT1 deacetylates KLF4 to activate Claudin-5 transcription in ovarian cancer cells. J. Cell. Biochem. 119, 2418–2426.
Zhao, H., et al., 2017. Resveratrol protects against spinal cord injury by activating autophagy and inhibiting apoptosis mediated by the SIRT1/AMPK signaling pathway. Neuroscience 348, 241–251.
Zhou, B., et al., 2014. CLOCK/BMAL1 regulates circadian change of mouse hepatic insulin sensitivity by SIRT1. Hepatology 59, 2196–2206.
Zhou, Y., et al., 2017. SIRT1/PGC-1alpha signaling promotes mitochondrial functional recovery and reduces apoptosis after intracerebral hemorrhage in rats. Front. Mol. Neurosci. 10, 443.